The Importance of Moisture Fluctuations and Wind Shear in Acoustic Backscatter in GATE

JOHN E. GAYNOR

Wave Propagation Laboratory, Environmental Research Laboratories, NOAA, Boulder, CO 80302

(Manuscript received 6 December 1978, in final form 11 August 1979)

ABSTRACT

We explain, using *in situ* data, some of the mechanisms contributing to acoustic backscatter measured using an active, vertically pointing echosonde (acoustic sounder) mounted aboard ship in the tropical Atlantic. Averaged tethered-sonde profiles indicate that the substantial wind shear through the low-level stable layer in the wake of precipitating convection contributes to the acoustic backscatter from this layer. The undisturbed top of the mixed layer shows much weaker shear and no echo, although the average stabilities are nearly the same in the undisturbed and wake cases. Combining theory with data provides an explanation of the importance of moisture in acoustic backscatter. In the suppressed mixed layer (little or no precipitating convection) the contribution to the backscatter due to moisture (C_e^2) approaches a factor of 3 greater than temperature fluctuations alone (C_T^2). In the disturbed boundary layer (organized convection) and moderately disturbed boundary layer (isolated convection), the moisture contributes less than 20%. Except near the top and near the bottom of the suppressed mixed layer, the co-fluctuations of moisture and temperature (C_{eT}) contribute immaterially. The categorized profiles of C_T^2, C_e^2 and C_{eT} do not exhibit clear tendencies toward $Z^{-4/3}$ slopes predicted by other authors.

1. Introduction

An atmospheric echosonde (acoustic sounder) installed aboard the NOAA research ship *Oceanographer* and deployed in the tropical Atlantic during the GARP Atlantic Tropical Experiment (GATE) from late June through September 1974, provided a unique opportunity to study the effects of moisture fluctuations on acoustic backscatter. Wind shear can create and destroy small-scale (0.01–10 m) temperature and moisture gradients. Acoustic backscatter responds very sensitively to these gradients. Because the vertical thermal and moisture stratification show little diurnal variation in the boundary layer, GATE provided an opportunity to isolate the effect of wind shear on acoustic backscatter. Strong wind shears due to vertical momentum transports and horizontal mesoscale pressure-gradient wind accelerations in the vicinity of precipitating convection led to large horizontal and temporal variability in the effects of shear on acoustic scatter.

The work of Tatarskii (1971) showed that, ordinarily, temperature fluctuation or equivalently, the structure parameter C_T^2, accounts for at least 98% of the acoustic backscatter. However, Friehe *et al.* (1975), Friehe (1977) and Wesely and Hicks (1978) have more recently shown that moisture fluctuations and correlated temperature and moisture fluctuations sometimes become large within atmospheric boundary layers over a warm water surface. Wesely (1976) developed a simple theory to take into account these moisture fluctuations (C_e^2) and temperature and moisture co-fluctuations (C_{eT}) in acoustic backscatter. Following discussions of the data sources and of the shear versus stability effects in acoustic backscatter, we apply NOAA DC-6 aircraft turbulence data from GATE to Wesely's theory, and show that moisture fluctuations contribute significantly to acoustic backscatter in a moist tropical marine mixed layer, amounting to most of the intensity under some conditions.

2. Data sources

a. Echosonde (acoustic sounder)

Mandics and Owens (1975) describe the operation of the echosonde installed aboard the *Oceanographer* and deployed during GATE. Mandics *et al.* (1975), Mandics and Hall (1976), Gaynor and Mandics (1978) and Gaynor (1978a,b) discuss the various aspects of the monostatic echosonde facsimile data from GATE, in some cases using surface and tethered *in situ* sonde data for comparison.

Fig. 1 presents an example of an echosonde facsimile recorded during the passage of organized precipitating convection. The vertical dark echoes near the bottom of the record before 1820 GMT represent warm, moist, thermal plumes rising from the warm sea surface. Intermittent rain noise begins after 1820. At around 2330, more horizontally stratified but wavey echoes appear, centered near

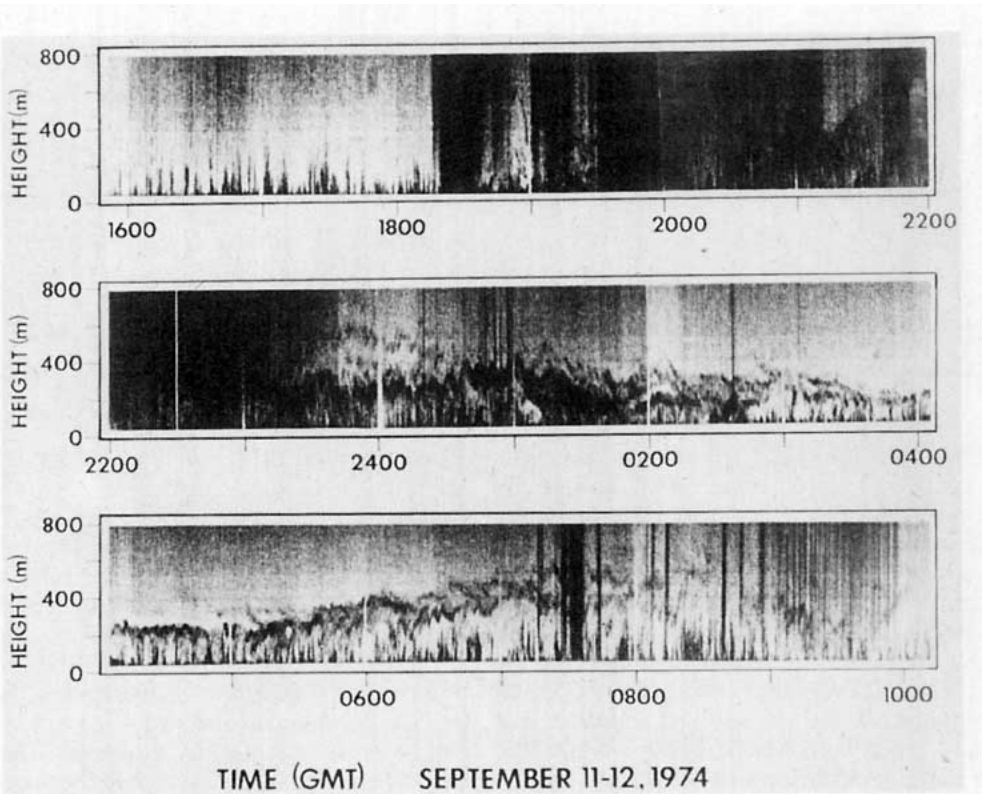

FIG. 1. An acoustic facsimile recorded during the passage of organized precipitating convection.

200 m. The echoes weakly persist until 1000 with plume echoes beneath them. Gaynor and Mandics (1978) have shown that these echoes represent regions of enhanced temperature stability and moisture gradients.

Interpretation of GATE acoustic records such as that in Fig. 1 requires *in situ* data. To understand the backscattering mechanism in this moist environment, we take advantage of the tethered sonde data from the *Oceanographer* and the NOAA DC-6 aircraft turbulence probe data from flights within the mixed layer (below 600 m).

b. Aircraft data

Bean *et al.* (1972), Brown *et al.* (1974) and Bean *et al.* (1975a,b, 1976) have documented the performance of the NOAA DC-6 gust probe turbulence measuring system. The system flew mainly within the mixed layer during GATE. The data used in this study were recorded from the radio-frequency refractometer measuring fluctuations in humidity (McGavin and Vetter, 1965), and from a double-bead thermister measuring fluctuations in temperature. Pressure transducers provided information on aircraft height.

Low-pass filtering of the turbulence data at 4.5 Hz provided a horizontal resolution of about 30 m (Grossman and Bean, 1973). The instrumental errors were approximately 2% for humidity fluctuations and 5% for temperature fluctuations.

c. The tethered sonde

The Boundary Layer Instrument System (BLIS) provided high-resolution profiles from the surface to 1 km during GATE. The composite data from this system aboard the *Oceanographer* were used to calculate wind shear and stability gradients discussed in the next section. A typical ascent/descent combination took ~20 min to complete.

Burns (1974) describes the BLIS instrumentation and its design specification for GATE in detail and Ropelewski (1976) presents an error analysis of the system. Gaynor and Ropelewski (1979) give examples of the use of GATE BLIS profile data normalized by mixed-layer height and averaged according to categorized echosonde facsimile records. The categorization scheme identified three different occurrences on the records: undisturbed [thermal plumes and perhaps a few of the weaker "hummocky" echoes described by Gaynor and Mandics (1978)], gust front or gravity current (low-level wavey echoes), and the storm wake (plumes capped by a low-level stable layer).

3. Wind shear and acoustic backscatter

Between 1820 and 2345 GMT on Fig. 1, rain noise hides most of the echoes. The time period between

TABLE 1. Stabilities and wind shears for the composite undisturbed and wake cases. The numbers of profiles are in parentheses and the σ's are the standard deviations.

	Phase II		Phase III		Average	
	Undisturbed	Wake	Undisturbed	Wake	Undisturbed	Wake
$(\overline{\partial\bar{\theta}_v/\partial Z})$ $\times 10^{-3}$ (K m^{-1})	3.8 (21)	3.0 (8)	3.7 (78)	4.0 (31)	3.7 (99)	3.8 (39)
σ ($\times 10^{-3}$)	2.7	1.1	2.9	2.6	2.8	2.0
$(\overline{\partial\tilde{U}/\partial Z})$ $\times 10^{-3}$ (s^{-1})	10.8 (21)	14.9 (8)	7.6 (67)	15.5 (27)	8.3 (89)	15.4 (35)
σ ($\times 10^{-3}$)	8.6	12.2	7.5	8.9	8.1	10.7

2330 and 1000 GMT, following the rain and up to the time in which the stable layer echo essentially disappears, exemplifies the storm "convective wake." The lowest stable layer echo delineates the top of the mixed layer. Previous to the onset of the rain (before 1820), no stable layer echo appears, even though the top of this "undisturbed" mixed layer averages between 500 and 600 m (Report of the U.S. GATE Central Program Workshop, 1977), well within the range of the echosonde. Because the GATE mixed layer was "undisturbed" about 70% of the time (Gaynor and Ropelewski, 1979), the top of the mixed layer does not often appear on the facsimile records. In terms of echosonde facsimile records, Gaynor and Ropelewski (1979) define "undisturbed" situations when no precipitation noise and no stable layer echoes appear on the records; i.e., when only plume echoes are evident.

Tatarskii (1971) and, in their review article, Brown and Hall (1978) clearly indicate that acoustic scatter requires turbulence. Substantial temperature gradients can exist without turbulence. In contrast, strong turbulence due to wind shear can exist with small potential temperature gradients. In both situations, little or no acoustic backscatter will occur.

Table 1 summarizes vertical virtual potential temperature gradients ($\partial\bar{\theta}_v/\partial Z$) and wind shear information from composite BLIS profiles indicating undisturbed conditions (no mixed-layer top visible on the acoustic facsimile records) or storm wake conditions (a clearly visible stable layer). The numbers of individual profiles used to make the composites are in parentheses in Table 1 with the standard deviations (σ) for each category tabulated beneath. We used the profiles from Phases II (mid-July to mid-August) and III (September) of GATE only because the acoustic facsimile records from Phase I did not always represent good quality. We calculated the gradients through a 10 mb layer. In the undisturbed cases, mixed layer tops and transition layers were visually identified from BLIS potential temperature and moisture profiles and the 10 mb regions were centered on the transition layers. The darkest stable layer appearing on the acoustic facsimile records at the times of the BLIS profiling dictated the location of the vertical gradients in the wakes.

The averages of $\partial\bar{\theta}_v/\partial Z$ for the two phases of GATE in Table 1 show no substantial difference in stability between the undisturbed and wake categories. To indicate the effect of moisture on stability, $\partial\bar{\theta}/\partial Z$ (not shown) was ~50% larger in the mean than $\partial\bar{\theta}_v/\partial Z$ for the two categories and the two phases of GATE, and also showed no significant difference between the categories. However, the wind shear appears nearly twice as large in the wake case. Even with the large standard deviations in the wind shear, the difference between the two categories is statistically significant at the 90% confidence level in the average. The data in Table 1 clearly support the ideas of Brown and Hall (1978) and provide an explanation for the lack of acoustic backscatter at the top of the undisturbed mixed layer.

4. Moisture fluctuations and acoustic backscatter

a. Theory

Wesely (1976) has provided the theoretical background. I have followed his notation and presented only those results pertinent to this analysis.

In homogeneous turbulence, Tatarskii (1971) expresses the structure function parameter for refractive index n as

$$C_n^2 = (2\overline{m^2} - 2\overline{m_1 m_2})/r^{2/3}, \quad (1)$$

where $m \equiv n - \bar{n}$, the overbar indicates a time average, and r represents the distance between m_1 and m_2. Tatarskii assumes that n is measured within the inertial subrange.

After beginning with the definition of acoustic refractive index and including the effect of moisture on the speed of sound, Wesely derives the following relations accurate to second order:

$$C_n^2 = [C_T^2/(4\overline{T^2})]\alpha_a^2, \quad (2a)$$

$$\alpha_a^2 = 1 + r_{eT}\left(\frac{2DC_e\bar{T}}{C_T\bar{p}}\right) + \left(\frac{DC_e\bar{T}}{C_T\bar{p}}\right)^2, \quad (2b)$$

where $r_{eT} = C_{eT}/(C_e C_T)$ and C_{eT} represent the crossed structure parameter of temperature (T) and vapor pressure (e). Because C_{eT} can become negative, we change Wesely's notation by not squaring the parameter to avoid an imaginary square root. $\bar{T}$ and $\bar{p}$ are the mean temperature and pressure, respectively, and $D \approx 0.318$. Various assumptions used in deriving (2) include ignoring the temperature dependency of the ratio of specific heats of constant pressure to constant volume, $e \ll p$, where p represents the total atmospheric pressure, and letting deviations from the means of e, p and T be much less than the means themselves. To adhere to Wesely's notation, we will leave the structure parameter for moisture in terms of vapor pressure. For completeness,

$$\frac{C_e^2}{C_q^2} = \left(\frac{R_w T}{10^5}\right)^2 \tag{3}$$

relates C_e^2 to C_q^2, the structure parameter in units of $(\text{g m}^{-3})^2\ \text{m}^{-2/3}$, where R_w represents the individual gas constant for water vapor.

Note that (2a) relates the acoustic refractive index parameter for acoustic backscatter in a dry atmosphere (Tatarskii, 1971) times a "correction" term (α_a^2) for moisture. Measurements in the next section clearly show that this correction is large in the moist GATE mixed layer.

We calculated the structure parameters C_T^2, C_e^2 and C_{eT}, as well as the mean quantities $\bar{T}$ and $\bar{p}$, from aircraft data. The retrieval of the structure parameters began with calculation of aircraft spectra of T and e, and cospectra of T and e for selected flights within the mixed layer each of 7 min duration. Within the inertial subrange Wyngaard *et al.* (1971) have established that

$$\Phi_T(k_1) = 0.25 C_T^2 k_1^{-5/3}, \tag{4}$$

where $\Phi_T(k_1)$ represents the average one-dimensional power spectrum and k_1 the wavenumber component in the streamwise direction. Similar relations hold for C_e^2 (Friehe *et al.*, 1975) and C_{eT} (Wyngaard *et al.*, 1978). When using aircraft data,

$$k_1 = \frac{2\pi f}{\bar{U}}, \tag{5}$$

where f represents the temporal frequency and $\bar{U}$ the aircraft speed ($\sim$100 m s^{-1}).

The relations presented in this section set the stage for measurements of α_a^2 and its components so that we may decide on the importance of each contributor to the moisture correction. The prolific GATE aircraft data allowed derivations of profiles of pertinent terms in (2) through much of the mixed layer, stratified according to synoptic situation.

TABLE 2. Summary of 7 min aircraft data runs.

Category	Level (m)	Number of runs
Suppressed	30	7
	91	5
	182	7
	305	4
	427	3
Moderately disturbed	91	14
	153	7
	305	3
Disturbed	153	13
	305	2
	396	4
	457	4

b. *Analysis*

As mentioned in Section 2b, the effect of the low-pass filter began at about 4 Hz. The spectral density intensities of T and e and the cospectral density intensities of T and e were taken from the 2 Hz point. Nearly always, the inertial subrange of the three quantities began at 0.5 Hz or less. We did not include in the analysis the few occasions when the spectra and cospectra did not clearly exhibit inertial subranges at 2 Hz. Gaynor (1978a) presents some examples of spectra of T and e and their cospectra for two flight segments. Because the 2 Hz point represents scales of about 50 m encountered by the aircraft and we are trying to compare with the $\sim$0.1 m scales ($\sim$30 Hz for a stationary platform and 600 Hz for the aircraft) to which acoustic scatter is sensitive, it is essential to use only data within the inertial subrange. Furthermore, a surface layer analysis presented later depends on an inertial subrange formulation. Because of the two orders-of-magnitude extrapolation in frequency, errors in the structure functions calculated from even the averaged spectra could approach 50%.

The NOAA DC-6 aircraft log (Bean *et al.*, 1976) from GATE provided indications of the mission type for any given day and provided information on the type of synoptic weather the scientists expected. The mission scientist reported on the actual weather encountered. This information allowed for a rough categorization of the mixed layer according to the amount of convective precipitation encountered. Table 2 lists the three categories, the height above the sea surface and the number of 7 min flights for each height.

The categories separate as follows:

(i) Suppressed—no precipitating convection encountered in the entire day's mission.

(ii) Moderately disturbed—some precipitating convection encountered, but isolated and disorganized.

TABLE 3. Structure parameters and their standard deviations (in parentheses).

Category	Level (m)	Parameter $C_T^2 \times 10^{-7}$ ($K^2\ m^{-2/3}$)	$C_e^2 \times 10^{-5}$ ($mb^2\ m^{-2/3}$)	$C_{eT} \times 10^{-7}$ (K mb $m^{-2/3}$)
Suppressed	30	1.69 (±0.55)	2.20 (±0.55)	9.04 (±3.38)
	91	1.27 (±0.34)	0.84 (±0.36)	5.00 (±3.49)
	182	0.91 (±0.24)	0.63 (±0.26)	1.50 (±1.24)
	305	0.56 (±0.21)	1.40 (±0.56)	−0.74 (±0.27)
	427	2.85 (±1.35)	1.86 (±0.98)	17.85 (±8.59)
Moderately disturbed	91	2.04 (±1.66)	1.06 (±0.40)	1.76 (±1.41)
	153	2.89 (±2.60)	1.51 (±0.88)	−0.52 (±25.40)
	305	1.07 (±0.39)	1.20 (±0.65)	−0.57 (±1.50)
Disturbed	153	261.34 (±156.00)	3.37 (±1.74)	43.94 (±84.20)
	305	47.42 (±61.90)	1.33 (±0.14)	22.73 (±31.20)
	396	4.95 (±4.58)	1.28 (±0.90)	−1.50 (±0.29)
	457	0.82 (±0.06)	1.12 (±0.35)	−0.31 (±1.85)

(iii) Disturbed—regions of large-scale organized precipitating convection encountered.

The profiles in the moderately disturbed case are not well defined because we include only three levels (Table 2).

The categories in Gaynor and Mandics (1978) and Gaynor and Roplewski (1979) are based mainly on echosonde facsimiles recording a time-height cross section at a point. These data allow for a very detailed categorization scheme. The aircraft categories are much more general, being based on the type of weather activity encountered on a given data-gathering day. Therefore, the aircraft may encounter regions between precipitating cells in which the boundary layer is suppressed according to the acoustic classification even on fairly disturbed days. We make the assumption that on the days considered suppressed, an echosonde would show mainly plumes (with perhaps a few weak hummocks). The echosonde would show short-lived disturbances (gravity currents and wakes) with periods of suppressed activity on a moderately disturbed day. The hummocks would be most numerous on this day, also. Wakes with many gravity current occurrences would dominate a disturbed day. Even with the often large distances between the aircraft and the *Oceanographer*, the structures appearing on the acoustic facsimile records were quite consistent with these assumptions. The moderately disturbed category is a mixture of suppressed and weakly disturbed boundary layer through a combination of which the aircraft may fly during a particular run as it moves under isolated rainshowers. This category separates the more homogeneous (in terms of boundary-layer structure) suppressed category within which no rain occurs and the disturbed category within which the modification of the boundary layer due to precipitating convection dominates.

Given the 100 m s^{-1} ground speed of the aircraft, a 7 min run translates to a path ~42 km long. The 73 runs used in this analysis and listed in Table 2 thus represent a very large volume of sampled air.

Table 3 presents the structure functions for the three categories which are plotted in Figs. 2–4. The table also lists the standard deviations, some of which are quite large, indicating the variability between runs. The standard deviations vary considerably between categories and levels because of the different number of runs within each category and at each level (Table 2) and the effects of the aircraft flying through varying mixed-layer depths and in and out of isolated downdrafts associated with rainshowers. The latter presented particular problems in the moderately disturbed and disturbed categories.

Fig. 2 presents the C_T^2 profiles with a $Z^{-4/3}$ line shown for reference. The depth of the mixed layer averages between 550 and 600 m in the suppressed GATE boundary layer and is quite variable in the disturbed cases, with average mixed-layer depths decreasing to 250 m in the convective wakes (Report of the U.S. GATE Central Program Workshop, 1977; Gaynor and Mandics, 1978). Note from Fig. 2 that the C_T^2 profiles do not exhibit $Z^{-4/3}$ slopes. Wyngaard *et al.* (1971), using similarity arguments, derived a −4/3 slope for C_T^2 through most of the lower half of the free convective mixed layer. Pennell and LeMone (1974), however, show that the suppressed trade wind mixed layer does not exhibit free convection. Substantial wind shears probably account for the slopes smaller than $Z^{-4/3}$ in the suppressed and moderately disturbed cases. The disturbed case indicates a slope much larger than $Z^{-4/3}$. Free convection obviously does not dominate in this category, with the modifying influences of

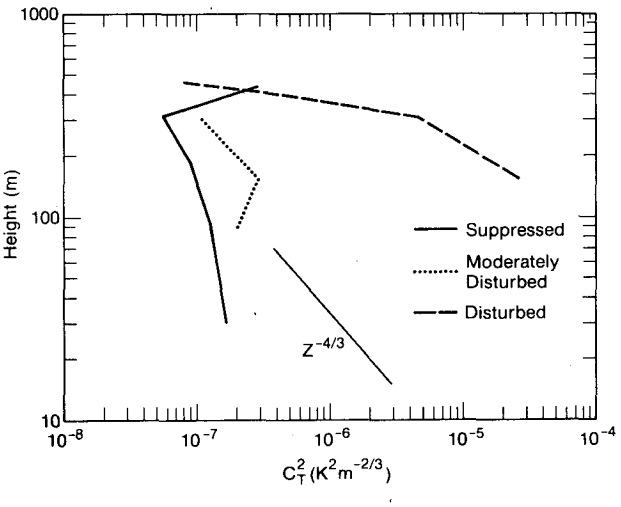

FIG. 2. Temperature structure function coefficient C_T^2 for the three categories. The $Z^{-4/3}$ line is plotted for reference.

convective precipitation-caused downdrafts and mesoscale sinking. As the post-precipitation section of the acoustic facsimile record in Fig. 1 indicates, strong low-level temperature turbulence in the region between the relatively warm ocean surface and the cool air from the downdrafts characterizes convective wakes. These wake events apparently dominate in the disturbed category creating a rather steep profile of C_T^2.

Fig. 2 shows that the magnitudes of C_T^2 between the suppressed and moderately disturbed categories do not look significantly different. Apparently, because of the isolated nature of the precipitating convection in the moderately disturbed category, the large, essentially suppressed regions between the clouds strongly influence the data.

Except for a few values in the disturbed category, the magnitudes of C_T^2 appear very small compared with those presented by many authors (e.g., Thomson *et al.*, 1978; Caughey *et al.*, 1978; Asimakopoulos *et al.*, 1976; Haugen *et al.*, 1975; Neff, 1975) who provide estimates of C_T^2 calculated from *in situ* and acoustic instrumentation in the range of 10^{-5} to 10^{-3} K^2 m$^{-2/3}$. The lowest range of magnitudes measured within stable layers is somewhat suspect because the accuracy of the above-mentioned instrumentation generally degrades as stability increases. Using a rather large data set from ships in the midlatitude oceans, Davidson *et al.* (1978) provide C_T^2 estimates within the same range, as does Friehe (1977) over warm water. Certainly, in the GATE suppressed mixed layer, temperature turbulence appears extremely small.

The formula presented by Friehe (1977) to parameterize C_T^2 in the boundary layer above the ocean in terms of easily measured quantities (i.e., the mean wind speed $\bar{U}$, the air-sea temperature difference ΔT and the air-sea water vapor density difference ΔQ) is

$$\frac{C_T^2 Z^{2/3}}{(\Delta T)^2} = 3.12 \times 10^{-3} (1 + 1.62X)^{-2/3} \quad (6a)$$

for the unstable atmosphere, where

$$X = [(Z\Delta T)/(\bar{U}^2)]\{1 + 0.212 \times [(\Delta Q)/(\Delta T)]\} \text{ K s}^2 \text{ m}^{-1}. \quad (6b)$$

Eq. (6b) includes the buoyancy effects due to moisture. Essentially, (6) combines the relation of Wyngaard *et al.* (1971) with the bulk formulation. If we use typical values from the GATE data from the suppressed surface layer (Z = 30 m, ΔT= 0.5 K, $\bar{U}^2$ = 25 m s^{-1} and ΔQ = 7.5 g m^{-3}) then, from (3), $C_T^2 = 3 \times 10^{-5}$ K^2 m$^{-2/3}$, which is two orders of magnitude larger than the 30 m suppressed value from Fig. 2. The formula obviously does not apply in the GATE mixed layer. However, Davidson *et al.* (1978) present evidence to show that, within both the stable and unstable surface layers above the midlatitude oceans, C_T^2 follows the parameterizations of Wyngaard *et al.* reasonably well.

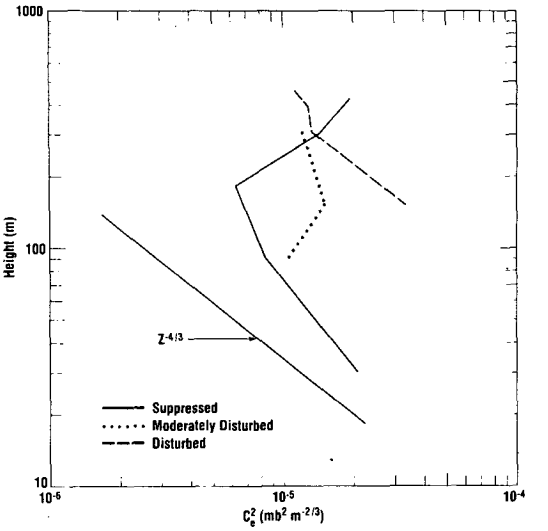

FIG. 3. As in Fig. 2 except for the moisture structure function coefficient C_e^2.

The C_e^2 profiles in Fig. 3 do not show appreciable differences in magnitudes between the categories. This result essentially agrees with the measurements of Zipser (1977) in organized convection and those of Gaynor and Ropelewski (1979) for a composite disturbed boundary layer. Cooling creates the major effect on the boundary layer during precipitation-caused downdrafts. The moisture changes little from ambient so we might expect only minor changes in moisture turbulence.

The suppressed C_e^2 profile in the lower mixed layer exhibits a tendency toward a $Z^{-4/3}$ slope. Wyngaard (private communication) calculated profiles of C_q^2 from the Air Mass Transformation Experiment (AMTEX) showing a somewhat ambiguous slope with some tendency toward $Z^{-4/3}$ in the lower half of the mixed layer. We must remember, however, that the AMTEX region exhibited sensible and latent heat fluxes at the sea surface many times larger than those in the GATE region because of the cold continental air overriding the warm Kuroshio Current. The AMTEX mixed layer exhibits more instability than the GATE mixed layer.

Notice in Fig. 4 that, except for the upper point in the suppressed profile, all three categories show slightly negative C_{eT} toward the top of the mixed layer. Deardorff (1974), using a numerical model of an entraining mixed layer, presented a profile showing a rather large negative correlation of θ_v' and q' in the upper half of the mixed layer, and Wyngaard *et al.* (1978) present AMTEX data with similar negative correlations. Essentially, drier and potentially warmer air above the top of the mixed layer

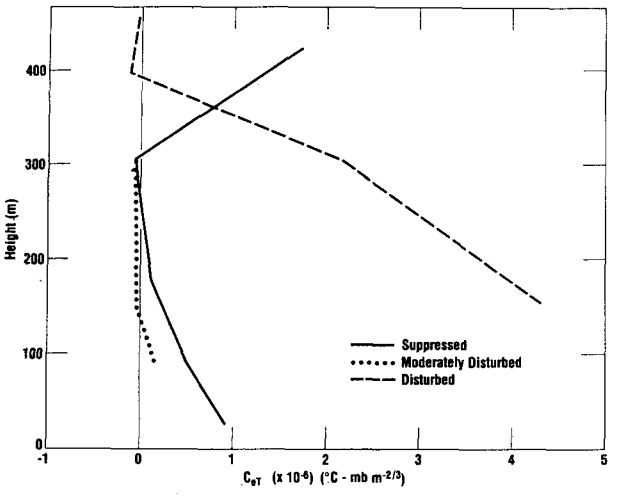

FIG. 4. The crossed structure function coefficient of moisture and temperature C_{eT}.

entrains downward. Note from (1) that a negative C_{eT} contributes negatively to α_a^2. In fact, if the second term on the right-hand side predominates over the other two terms, the moisture correction to C_n^2 can be less than 1. The discussion of Fig. 7 at the end of this section will indicate that the negative term only dominates, during a few specific runs, so that $\alpha_a^2 < 1$, but does not dominate in the average of all runs within each category.

Fig. 5 profiles the ratio $(DC_e\bar{T}/C_T\bar{p})^2$, the last term on the right in Eq. (2b), which measures the relative importance of moisture fluctuations to temperature fluctuations. The moisture fluctuations appear to predominate only at 305 m for the suppressed case. The moisture fluctuations are generally significant compared to the temperature fluctuations for both the moderately disturbed and the suppressed cases, but show little significance $[(DC_e\bar{T}/C_T\bar{p})^2 < 0.5]$ below 400 m for the disturbed category. This small ratio is mainly due to the relatively large C_T^2 values (Fig. 2) in the vicinity of the cool-air downdraft/sea surface interface rather than a decrease in C_e^2.

In the surface and free convective layers, Wesely and Alcaraz (1973) and Wesely (1976) have shown that

$$\frac{C_e\bar{T}}{C_T\bar{p}} = \frac{1}{(5.03|\beta|)}, \tag{7}$$

where $\beta = H/L_wE$, the Bowen ratio, H represents the sea surface sensible heat flux, and L_wE the sea surface latent heat flux. From *Oceanographer* measurements near the sea surface, $\beta = 0.1$ and, using (7), $C_e\bar{T}/C_T\bar{p} \approx 2$. At the 30 m level in the suppressed case $C_e\bar{T}/C_T\bar{p} \approx 3.4$ (Fig. 5). Even this approximate agreement is surprising considering the evidence discussed above that a free-convective, tropical mixed layer represents a dubious assumption.

Fig. 6 profiles the second term on the right-hand side of Eq. (2b) which represents the importance of C_{eT} to the backscatter. The term essentially shows how well the fluctuations of e and T are correlated relative to the individual fluctuations. Note the relative importance of this term (>0.5) in the lower and upper portions of the suppressed mixed layer and further note the relatively weak negative contribution near the upper portions of the moderately disturbed and disturbed boundary layers. The previously discussed entrainment of warm and dry air from above appears of minor importance in terms of its effect on acoustic backscatter in the latter two categories.

Fig. 7 combines the profiles in the previous figures. The error bars on the α_a^2 profiles in Fig. 7 represent the standard deviations of the individual runs at each level (Table 2). The standard deviations vary considerably between categories and levels for the reasons presented above.

Even with the large standard deviations in some cases, the differences in α_a^2 between the categories in Fig. 7 appear significant. The largest moisture effects in acoustic backscatter in the GATE mixed layer occur in the suppressed category. In the upper and lower portions of the mixed layer where the nearly equally large effects of C_e^2 and C_{eT} are combined (Figs. 5 and 6), $\alpha_a^2 \approx 3$. Through most of the convectively modified mixed layer in the disturbed category, the "correction" for moisture is less than 20%. We have previously discussed the reasons for the smaller moisture fluctuation effects in the disturbed case. Notice that, at least in the means, $\alpha_a^2 > 1$ even for the disturbed case. Only a few specific runs show the effect of a dominant $C_{eT} < 0$ term.

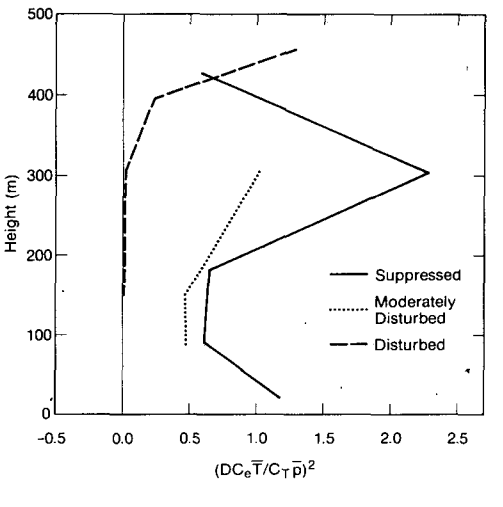

FIG. 5. The ratio $(DC_e\bar{T}/C_T\bar{p})^2$ showing the relative contributions of the structure function coefficients of moisture and temperature.

c. Applications

The analysis presented above enhances our ability to interpret monostatic acoustic facsimile records in a tropical environment. Improved interpretation allows for more efficient use of acoustic data to study boundary-layer structure in GATE.

Because of the relation between the acoustic refractive index structure parameter and the optical structure parameter (Tatarskii, 1971), the measurements presented here are useful in applications of optical propagation theories in the tropical boundary layer. In a lower signal-to-noise environment than was present on the *Oceanographer*, methods exist for calibration of monostatic echosondes (e.g., Neff, 1975, 1978) to remotely measure C_n^2. These measurements have never been made acoustically in the tropics. If measurements were made in a tropical boundary layer, the understanding of the moisture contributions to acoustic backscatter becomes imperative.

5. Summary and conclusions

Using BLIS profile data from the *Oceanographer* and NOAA DC-6 aircraft data, we have explained two aspects of acoustic backscatter in the GATE boundary layer: (i) that the top of the suppressed mixed layer was not delineated by the acoustic facsimile records but appeared clearly during precipitation wake regimes; and (ii) that moisture fluctuations and co-fluctuations of moisture and temperature contributed to the acoustic backscatter. The relatively large wind shear in the wakes explains (i). The moisture fluctuation component of acoustic backscatter is large, and in fact may predominate in the GATE mixed layer.

Because acoustic backscatter requires both turbulence and gradients in potential temperature for acoustic backscatter, a stronger wind shear regime provides stronger scatter given equal background potential temperature gradients. The turbulence continually creates and destroys microscale (0.01–10 m) temperature gradients, thereby enhancing acoustic backscatter.

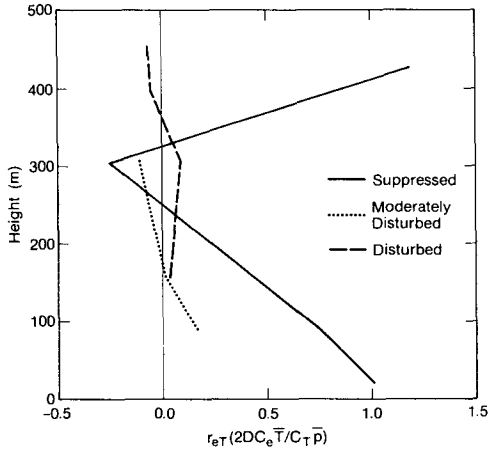

FIG. 6. The contribution of the correlation between moisture and temperature, $r_{eT}(2DC_e\bar{T}/C_T\bar{p})$.

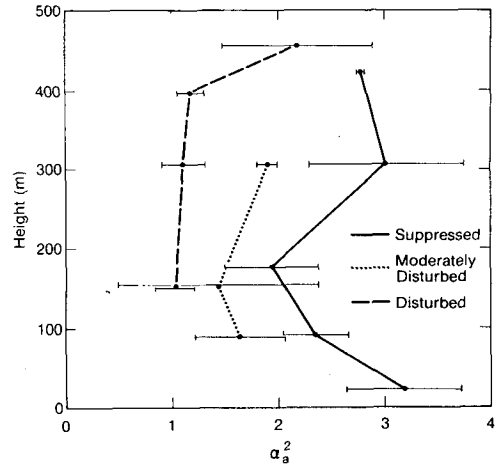

FIG. 7. The correction factor α_a^2 including all moisture fluctuation effects up to second order.

Following Wesely's (1976) theoretical development and supplying aircraft turbulence data, we found, in the suppressed and moderately disturbed categories especially, that the moisture fluctuations contribute importantly to acoustic backscatter. In fact, on the average, the contribution approaches a factor of 3 larger than the temperature contribution alone in the suppressed category. In the lower portion of the disturbed boundary layer, the moisture fluctuation contribution appears relatively small (<20%). The moisture fluctuations do not significantly change between suppressed and disturbed conditions, but the temperature fluctuations increase by about two orders of magnitude in the lower portion of the disturbed boundary layer. Except near the top and near the bottom of the suppressed mixed layer, the co-fluctuations of moisture and temperature contribute immaterially for the three categories.

The GATE acoustic sounder and supporting data provided a unique opportunity to study the wind shear effects on acoustic backscatter because of the relatively weak and constant potential temperature gradients. The wealth of aircraft data for the GATE mixed layer allowed an assessment of the moisture contribution to acoustic backscatter. This contribution actually dominated much of the time. We can place these results in context by mentioning that we have considered nearly the most moist boundary layer possible. In almost all other situations, especially over the continents, moisture contributions to acoustic backscatter would be insignificant.

Acknowledgments. The author gratefully acknowledges the data organization, computer programming assistance and data plotting provided by C. W. King and J. E. Birtwistle. The author also appreciates the assistance of R. F. Reinking and R. F. Hartmann in extracting the aircraft data from the tapes. Thanks are also extended to Professors R. McIlveen and D. Thomson of Pennsylvania State University for their critical reading of and suggestions on the final manuscript. The U.S. GATE Project Office supported the research.

REFERENCES

Asimakopoulos, D. N., R. S. Cole, S. J. Caughey and B. A. Crease, 1976: A quantitative comparison between acoustic sounder returns and the direct measurement of atmospheric temperature fluctuations. *Bound.-Layer Meteor.*, **10**, 137–148.

Bean, B. R., R. O. Gilmer, R. L. Grossman, R. E. McGavin and C. Travis, 1972: An analysis of airborne measurements of vertical water vapor flux during BOMEX. *J. Atmos. Sci.*, **29**, 860–869.

——, C. B. Emmanuel, R. O. Gilmer and R. E. McGavin, 1975a: Spatial and temporal variations of the turbulent fluxes of heat, momentum, and water vapor over Lake Ontario during IFYGL. NOAA Tech. Rep. ERL 313 WMPO 5, 57 pp.

——, ——, —— and ——, 1975b: The spatial and temporal variations of the turbulent fluxes of heat, momentum and water vapor over Lake Ontario. *J. Phys. Oceanogr.*, **5**, 532–540.

——, R. O. Gilmer, R. F. Hartmann, R. E. McGavin and R. F. Reinking, 1976: Airborne measurements of vertical boundary layer fluxes of water vapor, sensible heat and momentum during GATE. NOAA Tech. Memo. ERL WMPO-36, 83 pp.

Brown, E. H., and F. F. Hall, Jr., 1978: Advances in atmospheric acoustics. *Rev. Geophys. Space Phys.*, **16**, 47–110.

Brown, W. J., Jr., J. D. McFadden, H. J. Mason, Jr., and C. W. Travis, 1974: Analysis of the Research Flight Facility gust probe system. *J. Appl. Meteor.*, **13**, 156–167.

Burns, S. G., 1974: Boundary-layer instrumentation system. *Atmos. Tech.*, **6**, 123–128.

Caughey, S. J., B. A. Crease, D. N. Asimakopoulos and R. S. Cole, 1978: Quantitative bistatic acoustic sounding of the atmospheric boundary layer. *Quart. J. Roy. Meteor. Soc.*, **104**, 147–161.

Davidson, K. L., J. M. Houlihan, C. W. Fairall and G. E. Schacher, 1978: Observation of the temperature structure function parameter C_T^2 over the ocean. *Bound.-Layer Meteor.*, **15**, 507–523.

Deardorff, J. W., 1974: Three-dimensional numerical study of turbulence in an entraining mixed layer. *Bound.-Layer Meteor.*, **7**, 199–226.

Friehe, C. A., 1977: Estimation of the refractive-index temperature structure parameter over the ocean. *Appl. Opt.*, **16**, 334–350.

——, J. C. LaRue, F. H. Champagne, C. H. Gibson and G. F. Dreyer, 1975: Effects of temperature and humidity fluctuations on the optical refractive index in the marine boundary layer. *J. Opt. Soc. Amer.*, **65**, 1502–1511.

Gaynor, J. E., 1978a: Analysis of the disturbed boundary layer during GATE using acoustic sounder data. *Preprints 11th Tech. Conf. Hurricanes and Tropical Meteorology*, Miami Beach, Amer. Meteor. Soc., 242–246.

——, 1978b: Acoustic sounding in a moist tropical marine atmospheric boundary layer during GATE. *Preprints Fourth Symp. Meteorological Observations and Instrumentation*, Denver, Amer. Meteor. Soc., 410–414.

——, and P. A. Mandics, 1978: Analysis of the tropical marine boundary layer during GATE using acoustic sounder data. *Mon. Wea. Rev.*, **106**, 223–232.

——, and C. F. Ropelewski, 1979: Analysis of the convectively modified GATE boundary layer using *in situ* and acoustic sounder data. *Mon. Wea. Rev.*, **107**, 985–993.

Grossman, R. L., and B. R. Bean, 1973: An aircraft investigation of turbulence in the lower layers of a marine boundary layer. NOAA Tech. Rep. ERL 291 WMPO 4, 166 pp. [NTIS COM-74-50337].

Haugen, D. A., J. C. Kaimal, C. J. Readings, and R. Rayment, 1975: A comparison of balloon-borne and tower-mounted instrumentation for probing the atmospheric boundary layer. *J. Appl. Meteor.*, **14**, 540–545.

Mandics, P. A., and E. J. Owens, 1975: Observations of the marine atmosphere using a ship-mounted acoustic echo sounder. *J. Appl. Meteor.*, **14**, 1110–1117.

——, and F. F. Hall, Jr., 1976: Preliminary results from the GATE acoustic echo sounder. *Bull. Amer. Meteor. Soc.*, **57**, 1142–1147.

——, ——, E. J. Owens and D. Wylie, 1975: Observations of the tropical marine atmosphere using an acoustic echo sounder during GATE. *Preprints 16th Radar Meteorology Conf.*, Houston, Amer. Meteor. Soc., 257–259.

McGavin, R. E., and M. J. Vetter, 1965: Radio refractometry and its potential for humidity studies. *Humidity and Moisture*, Vol. 2, Reinhold Publ. Corp., 561–568.

Neff, W. D., 1975: Quantitative evaluation of acoustic echoes from the planetary boundary layer. NOAA Tech. Rep. 322–WPL 38, 34 pp. [NTIS PB-253 207].

——, 1978: Beamwidth effects on acoustic backscatter in the planetary boundary layer. *J. Appl. Meteor.*, **17**, 1514–1520.

Pennell, W. T., and M. A. LeMone, 1974: An experimental study of turbulence structure in the fair-weather trade wind boundary layer. *J. Atmos. Sci.*, **31**, 1308–1323.

Report of the U.S. GATE Central Program Workshop, 25 July–12 August 1977: National Center for Atmospheric Research, Boulder, 723 pp.

Ropelewski, C. F., 1976: An evaluation of the meteorological data from the GATE Boundary Layer Instrument System (BLIS). NOAA Tech. Memo. EDS-CEDDA-9, 24 pp. [NTIS PB-283-573].

Tatarskii, V. I., 1971: *The Effects of the Turbulent Atmosphere on Wave Propagation*. 471 pp. [NTIS NOAA TT 68-50464].

Thomson, D. W., R. L. Coulter and Z. Warhaft, 1978: Simultaneous measurements of turbulence in the lower atmosphere using sodar and aircraft. *J. Appl. Meteor.*, **17**, 723–734.

Wesely, M. L., 1976: The combined effect of temperature and humidity fluctuations on refractive index. *J. Appl. Meteor.*, **15**, 43–49.

——, and E. C. Alcaraz, 1973: Diurnal cycles of the refractive index structure function coefficient. *J. Geophys. Res.*, **78**, 6224–6232.

——, and B. B. Hicks, 1978: High-frequency temperature and humidity correlation above a warm wet surface. *J. Appl. Meteor.*, **17**, 123–128.

Wyngaard, J. C., Y. Izumi and S. A. Collins, Jr., 1971: Behavior of the refractive-index-structure parameter near the ground. *J. Opt. Soc. Amer.*, **61**, 1646–1650.

——, W. T. Pennell, D. H. Lenschow, and M. A. LeMone, 1978: The humidity-temperature covariance budget in the convective boundary layer. *J. Atmos. Sci.*, **35**, 47–58.

Zipser, E. J., 1977: Mesoscale and convective-scale downdrafts as distinct components of squall line structure. *Mon. Wea. Rev.*, **105**, 1568–1589.